

forms within soil profile (Pal & Mukhopadhyay, 1992; Singh et al., 2006) and in surface soils (Basumatary & Bordoloi, 1992; Sharma et al., 2009) was reported in India. Even field scale spatial variability of P fractions (Heilmann et al., 2005) and village level variability of K fractions (Chatterjee et al., 2015) using geostatistical tools were reported by several authors. But mapping of distribution of phosphorus and potassium fractions at farm scale using geostatistical technique has not been reported to date for precision nutrient management in India.

The objective of the present ^{carried out} research was to evaluate the status of soil phosphorus and potassium fractions, identifying its spatial dependency through spatial modeling and mapping of its spatial distribution using geostatistical tool in geographic information system (GIS)-environment at ICAR-IARI farm, New Delhi.

2. Material and methods

2.1. Site descriptions and soil sampling

The research work was conducted at farm of the ICAR-Indian Agricultural Research Institute (IARI) in New Delhi (77°8'40.48" - 77°10'28.07" East longitude, 28°37'21.97" - 28°38'58.74" North latitude). The farm has a total area of about 278 hectares and is divided into various administrative blocks (Fig. 1) and several crops are cultivated during *Monsoon* and *Rabi* seasons. A total of 288 soil samples from the farm were collected using grid sampling techniques of 100 m × 100 m distance at soil depth of 0-15 cm after harvesting of *Rabi* crops, 2010-11. The collected soil samples with proper tagging were air-dried, processed and sieved with 2 mm mesh for laboratory analysis.

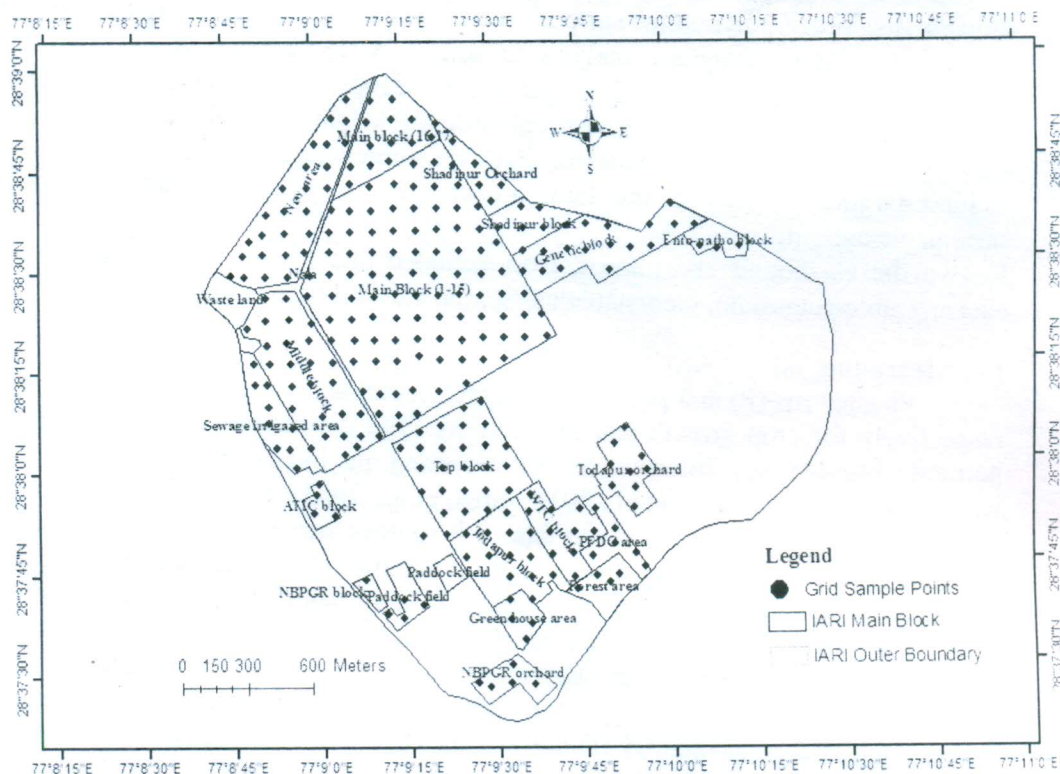


Fig 1. Location, major block and collected sample points at ICAR-IARI farm, New Delhi

2.2. Analysis of soil samples

Soil parameters such as soil pH in 1:2.5 ratio of soil & water suspension, soil organic carbon *i.e.* Walkley & Black carbon (WBC), calcium carbonate equivalent (CCE) (Piper, 1966), texture (Bouyoucos, 1962) and cation exchange capacity (CEC) (Page et al., 1982) were analyzed using standard methodologies mentioned within parenthesis. Soil phosphorus fractionation is a method for characterizing soil phosphorus availability without phosphorus speciation. Soil available phosphorus ($\text{NaHCO}_3\text{-P}$) was extracted by Olsen's extractants and phosphorus concentration in the extracted solution was measured by ascorbic acid method. The extraction procedure for several soil P-fractions involves the sequential P fractionation procedure with (i) 0.1N NaOH to extract non-occluded Al- and Fe-bound phosphorus, (ii) 1M NaCl and citrate-bicarbonate (CB) to extract P sorbed by carbonates during the previous NaOH extraction, (iii) citrate-dithionite-bicarbonate (CBD) to extract P occluded within oxides and hydrous oxides of iron (Fe), and (iv) 1N HCl to remove Ca-bound P (Page et al., 1982). These four phosphorus fractions are represented as NaOH extractable phosphorus (NaOH-P), citrate-bicarbonate extractable phosphorus (CB-P), citrate-bicarbonate-dithionite extractable phosphorus (CBD-P) and HCl extractable phosphorus (HCl-P). Estimation of CB and CBD extractable phosphorus was also followed by the standard method (Page et al., 1982). The solution P concentration was determined with reduction of phospho-molybdic acid complex by ascorbic acid reduction method (Watanabe & Olsen, 1965).

Processed soil samples were used for analysis *viz.* plant available K ($\text{NH}_4\text{OAc-K}$) extracted by shaking 5 g soil with 25 mL of 1N neutral ammonium acetate for 5 minutes (Hanway & Hiedal, 1952) and reserve K or 1N $\text{HNO}_3\text{-K}$ by boiling 2.5 g soil with 1N HNO_3 for 10 minutes (Wood & De Turk, 1940) and the non-exchangeable K was calculated by subtracting 1N $\text{NH}_4\text{OAc-K}$ from 1N $\text{HNO}_3\text{-K}$.

2.3. Statistical and geo-statistical Analysis

Exploratory data analysis of soil P- & K- fractions in the farm was conducted. Trend analysis of soil attributes was conducted in Arc-GIS software. Semivariogram analysis of soil P- & K-fractions was conducted in geostatistical wizard of the GIS software. The prediction maps of soil P- & K-fractions were created using ordinary kriging interpolation technique.

3. Results and discussion

3.1. Descriptive statistics of P- and K- fractions

Descriptive statistical parameters of soil P- and K- fractions were provided in Table 1. The soil available P content ($\text{NaHCO}_3\text{-P}$) was high with mean value of 22.4 mg kg^{-1} . The soil P-fractions at IARI farm followed the sequence $\text{HCl-P} (214.7 \text{ mg kg}^{-1}) > \text{CB-P} (40.8 \text{ mg kg}^{-1}) > \text{NaOH-P} (32.8 \text{ mg kg}^{-1}) > \text{CBD-P} (31.4 \text{ mg kg}^{-1})$ on average data basis. It indicated that indiscriminate use of phosphorus and potassium fertilizer in the intensively cultivated farm accelerated P fixation, subsequently leading to P fertility build-up. Crops can easily absorb the available soil phosphorus from soil solution phase (intensity factor) and it could be replenished by their quantity factors (Mengel & Kirkby, 1987). Quantity factors of soil phosphorus indicate total quantity of phosphorus in soils and here, inorganic phosphorus such as Ca-bound P, non-occluded Al- & Fe-P and occluded P were major constituents of the quantity factor. Soil available K content in the farm was high with average of 157.1 mg kg^{-1} . The non-exchangeable-K content of maximum soil samples in the farm were also grouped into high class ($600\text{-}1200 \text{ mg kg}^{-1}$) with mean value of 1077 mg kg^{-1} . Hence, quantity factor of K *i.e.* non-exchangeable-K could also supply on long term basis to intensity factor *i.e.* plant available K form while its value decreases below threshold level over plant K uptake, K leaching on irrigation or rainfall in light textured soil.

3.2. Surface trend analysis

The spatial data of soil P & K fractions were analysed for identification of surface trend. There was global trend observed for CBD-P & HCl-P fractions (Fig 2). CBD-P value increased from West to East direction and North to South direction. The northern and north western side of the farm had lower CBD-P values and eastern and south eastern side of the farm had higher values. The trend of CBD-P fraction was fitted with first order polynomial and this trend was removed before geostatistical analysis. Values of HCl-P fraction decreased from West to East direction and North to South direction. The northern and north western side of the farm had high values of HCl-P fractions and the southern and south eastern side of the farm had low values. The trend of HCl-P fraction was fitted with first order polynomial and this trend was removed before geostatistical analysis.

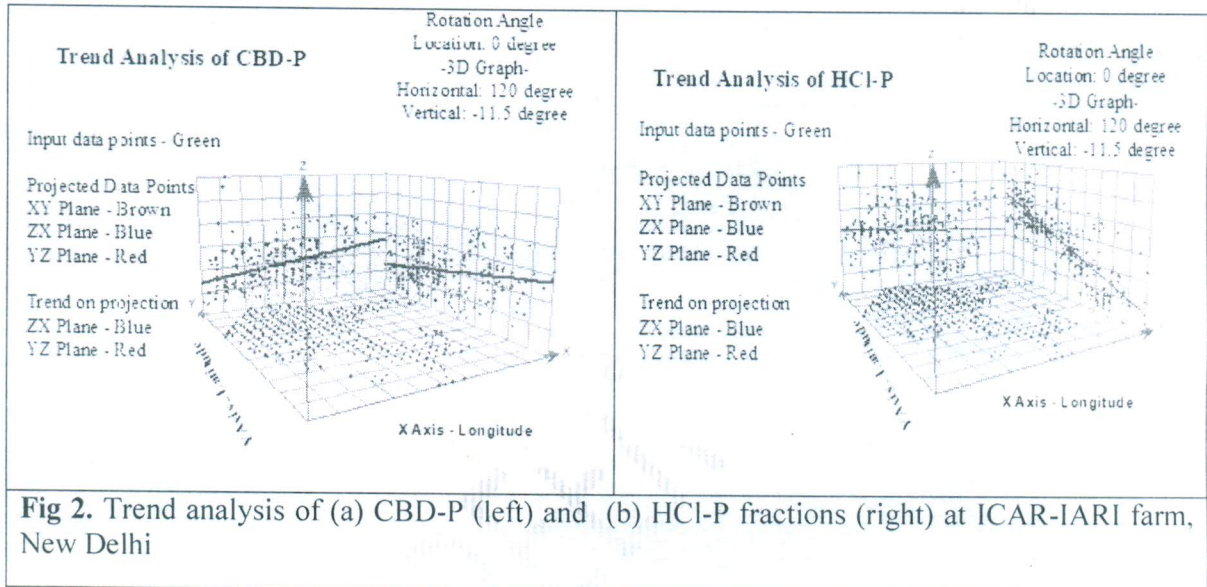


Fig 2. Trend analysis of (a) CBD-P (left) and (b) HCl-P fractions (right) at ICAR-IARI farm, New Delhi

3.3. Semivariogram analysis and spatial structure

The semi-variograms of soil P-fractions viz. $\text{NaHCO}_3\text{-P}$, NaOH-P , CB-P , CBD-P and HCl-P content and K-fractions viz soil available K and non-exchangeable K content are shown in Fig. 3. In the semivariogram, binned semivariance, average semivariance to particular lag class and best fitted semivariogram model for soil P-& K-fractions were shown in the corresponding graph. Key parameters of the best fit semi-variogram *i.e.* nugget, sill and parameter range are given in Table 4. The largest point pair distance in the present study was 2909 m and as thumb rule, active lag distance (*i.e.* lag size multiplied by no of lag size) varied from 1/3 to 1/2 (900-1500 m) of the longest point pair distance. The best fitted semivariogram model among spherical, exponential, gaussian, linear and linear-to-plateau models was selected from least residual sum of square value (RSS). In this study, the optimal semivariogram model of $\text{NaHCO}_3\text{-P}$ & CB-P content was exponential, whereas NaOH-P , $\text{NH}_4\text{OAc-K}$, non-exchangeable-K were best fitted to spherical models. After trend removal, the semi-variogram of CBD-P and HCl-P fractions were also best fitted in spherical model. The selection of best fitted semivariogram had influence on the prediction of soil P- & K-fractions at unsampled location, particularly when the curve significantly differed in shape near the origin.

3.4. Spatial distribution of phosphorus and potassium fractions

The spatial distribution of phosphorus fractions (Fig 4) at ICAR-IARI farm were categorized into different classes. The bulk of IARI farm had high level of plant available soil phosphorus ($> 11.2 \text{ mg kg}^{-1} \text{ P}$) (Fig 4a). The northern corner, western side, eastern fringe and patches in Todapur block and Paddock field of the farm had very high level ($22.3 - 113.6 \text{ mg kg}^{-1}$) of soil available P. The high level of plant available soil phosphorus was accumulated in the crop field due to continuous cultivation with P-fertilization.

In case of NaOH-P *i.e.* non-occluded Al- & Fe-bound P (Fig 4b), bulk of the farm were grouped under classes of $0.7 - 25 \text{ mg kg}^{-1} \text{ P}$ and $25-50 \text{ mg kg}^{-1} \text{ P}$. The western side of the farm under sewage irrigation had high level ($50-100 \text{ mg kg}^{-1}$) of NaOH-P. For occluded phosphorus within crystalline iron oxides and hydroxides *i.e.* CBD-P (Fig 4d), the major area of the farm had been grouped under first three classes (upto $45.5 \text{ mg kg}^{-1} \text{ P}$). The south and south eastern area of the farm had comparatively higher value of CBD-P, indicating presence of oxides and hydroxides of iron and aluminium. Distribution of CBD-P in the farm was related with free oxides distribution in different soil serieses as reported by (AIS & LUS, 1976). Amorphous ferri- allumino-silicate (AFAS), allophone and imogolite content were reported as higher quantity than ferrihydrite in Inceptisols of ICAR-IARI farm (D. Chatterjee et al., 2014). These amorphous or short range minerals contributed towards higher non-occluded soil phosphorus than occluded soil phosphorus.

The distribution of CB-P in the farm was depicted in Fig 4c and bulk of the farm had $25-50 \text{ mg kg}^{-1} \text{ P}$. The spatial distribution of HCl-P *i.e.* Ca-bound soil P fraction (Fig 4e) at the farm followed opposite pattern of CBD-P distribution. The soil at northern and north eastern fringe of IARI farm had HCl-P of $200-385.4 \text{ mg kg}^{-1}$ and subsequently, the value declined in southern direction. The soil of southern portion contained $67.3-200 \text{ mg kg}^{-1}$ of HCl-P. The higher HCl-P in northern portion would be due to presence of high active calcium carbonate equivalent and high phosphorus fertilization in the intensively cropping system for long term basis (Gorai, 2015). The lower HCl-P in southern portion might be due to less fertilization in orchard of Top block, Todapur block, kisan mela ground and forest area. It might be the facts that the Ca-P compounds were converted into Al-P and sesquioxide bound P with maturity of soils (Singh et al., 2003).

The spatial variability map of available K was depicted in Fig 4f. Intermediate levels of soil available K ($54 - 125 \text{ mg kg}^{-1}$) were found in the southern part of the farm, excluding Todapur orchards, forest area, NBPGR block & Paddock field. The north corner, fallow land and a part within the Main Block had very high levels of available K ($>200-400 \text{ mg kg}^{-1}$). However, the rest of the farm showed high levels of available K ($125-200 \text{ mg kg}^{-1}$). The prediction map of soil non-exchangeable - K (Fig 4g) displayed that bulk of the farm soils had high level ($600-1200 \text{ mg kg}^{-1}$) of non-exchangeable K and a few patches within Main Blocks, WTC & PFDC area and NBPGR orchard area had very high level ($>1200 \text{ mg kg}^{-1}$). The spatial distribution of soil available K & non-exchangeable K at the farm had similarity with distribution of particle size fractions & CEC (Gorai et al., 2015). The high and very high level of non-exchangeable potassium in the farm was attributed by the presence of mica as dominant clay mineral with associated minerals of kaolinite, vermiculite or chlorite and interstratified minerals (Mohanty, 1997). The highest content of mica in soils developed on alluvium was due to micaceous nature of alluvium in Yamuna River. Similarly, non-exchangeable K reserves in illite-rich alluvial soils were reported as highest quantity (Subba Rao et al., 1993).

3.5. Cross validation of prediction map

The generated spatial distribution maps of soil phosphorus and potassium fractions through ordinary kriging and ordinary kriging after lognormal transformation of data were evaluated through cross validation and was provided in Table 5. Mean prediction error (MPE), root mean square error (RMSE), average standard error (ASE), mean standardized error (MSE) and root mean square standardized error (RMSSE) were used for selection of the best kriging techniques. MPE determines the degree of bias in the estimates, RMSE measures the error size and ASE is associated with standard error of prediction. Prediction model is good if MPE becomes near to zero and RMSE value is smaller & closer to ASE. In respect to MSE & RMSSE, prediction model is good if MSE becomes near to zero and RMSE value is closer to one. From analysis of cross validation error, it was observed that ordinary kriging technique was better for $\text{NaHCO}_3\text{-P}$, NaOH-P , CB-P , $\text{NH}_4\text{OAc-K}$ and non-exchangeable - K than lognormal ordinary kriging. For CBD-P & HCl-P , ordinary kriging after trend removal performed better than ordinary kriging without trend removal.

Table 5 Evaluation performance of kriged map of soil properties through cross validation

| Soil attributes | Interpolation techniques* | Mean prediction error | Root mean square error | Average standard error | Mean standardized Error | Root Mean square standardized error |
|--------------------------------|---------------------------|-----------------------|------------------------|------------------------|-------------------------|-------------------------------------|
| $\text{NaHCO}_3\text{-P}$ | OK | -0.1161 | 11.98 | 11.71 | -0.0068 | 1.0213 |
| | OK_{LG} | -0.2324 | 12.14 | 12.17 | -0.0246 | 1.0509 |
| NaOH-P | OK | -0.0051 | 19.10 | 19.45 | -0.0005 | 0.9815 |
| | OK_{LG} | 0.3700 | 18.85 | 21.09 | 0.0274 | 0.8276 |
| CB-P | OK | -0.1352 | 16.06 | 15.11 | -0.0080 | 1.0593 |
| | OK_{LG} | -0.4769 | 15.76 | 14.80 | -0.02713 | 1.0730 |
| CBD-P | OK | -0.0606 | 6.37 | 6.36 | -0.0088 | 1.0013 |
| CBD-P (Detrended) | OK | -0.0727 | 6.38 | 6.37 | -0.0107 | 1.0003 |
| HCl-P | OK | -0.2122 | 42.05 | 38.68 | -0.0035 | 1.0837 |
| HCl-P (Detrend) | OK | -0.1367 | 42.20 | 39.73 | -0.0013 | 1.0592 |
| $\text{NH}_4\text{OAc-K}$ | OK | -1.8028 | 76.43 | 68.23 | -0.0214 | 1.0989 |
| | OK_{LG} | -2.0932 | 76.04 | 65.92 | -0.0332 | 1.1841 |
| Non-Exch. K | OK | -0.3144 | 116.40 | 113.72 | -0.0005 | 1.0255 |
| | OK_{LG} | -0.3679 | 116.18 | 110.90 | -0.0057 | 1.02837 |

*OK – ordinary kriging, OK_{LG} – Lognormal ordinary kriging,

4. Conclusion

Soil available P content at ICAR-IARI farm, New Delhi had medium to very high level. Ca - bound P-fraction was found as the major P fraction at ICAR-IARI farm, followed by non-occluded Fe- & Al- bound P and occluded Fe- P. Soil available K in the farm had medium to very high level and non-exchangeable K content was high to very high level. Available phosphorus was positively and significantly correlated with all P fractions and soil organic carbon content. Thematic mapping of soil P and K fractions indicated both plant